Proceedings of the 7th JFPS International
Symposium on Fluid Power, TOYAMA 2008
September 15-18, 2008

P1-48

A NOVEL LEAKAGE DETECTION AND LOCALIZATION METHOD BASED ON INFRARED THERMOGRAPHY

Nan GE, Guangzheng PENG

Department of Automatic Control, School of Information Science and Technology
Beijing Institute of Technology
5 South Zhongguancun Street, Beijing, 100081, China
(E-mail: genan@bit.edu.cn)

ABSTRACT

The common ways used to find leak include traditional bubbling test, ultrasonic positioning and helium mass-spectrometer detection, etc. However, each of them has deficiencies of varying degrees, especially low-efficiency in bubbling and mass spectrometry means and poor anti-jamming capability in ultrasonic means. In order to search a better approach to do this job, a new method is introduced in this paper, which is based on infrared thermography. In the experiment, test vessel is firstly aerated with absolute pressure of 0.6-0.7 Mpa and then the temperature field surround the vessel is monitored and acquired by an IR camera. On account of leakiness, compressed air expanses from the leak hole to ambient and heat-absorption effect has taken place around it on the basis of Joule-Thomson Effect, so the temperature difference between the leak area and normal area will be reflected in the thermal images. Moreover, Freon cooler is also set in the pneumatic circuit for the sake of enhancing the phenomenon. During the test, several frames of thermal images in time sequence are transferred to the computer for pre-processing and fusion operating by the use of local entropy difference algorithm. From results, it is shown that the method achieves a good resolution and sensitivity in the application of air-leakage detection and localization. Some modeling and simulating work by finite element analysis is also carried out in this paper.

KEY WORDS

Leak Detection, Leak Localization, Joule-Thomson Effect, Finite Element Analysis, Infrared Image Processing

INTRODUCTION

In most industrial processes, air-leakage detection and localization of vessels is an essential link of manufacturing. With the development of manufacturing technology, more and more requirements about not only leak detection but also leak localization are put forward. Most of current localization researches focus on leakage of petroleum and natural gas pipeline, while little new work was done to vessels' leak. Generally, there are three traditional ways to find tiny leak on the vessels[1]. The first one is air bubbling test which needs the target to soak in water, so it is constrained to be used for objects with immersion forbiddance. The second is mass spectrometry which has the highest precision in detections, but its broad application is hindered by low-efficiency. The third one is ultrasonic positioning which is interfered easily by noise. Due to the disadvantages of low-efficiency and poor anti-jamming capability in traditional vessels' leakage localization

approaches, a novel method was proposed in this paper. Along with the gradual perfection of infrared technology, thermography has been increasingly used in leakage detection and localization field. This paper utilizes a computer based system which contains a specific pneumatic circuit in conjunction with an on-line infrared camera to determine the air-tightness of a test vessel. A mathematical model has been set for subsequent leakage localization processing by analyzing leak throttle and heat transfer process around the leak. Moreover, the finite element analysis (FEA) was used to do some simulations. In order to find the leak point in the thermal images, a set of means based on local entropy difference algorithm has been adopted.
Experiment shows that the simulation fits the result well and verifies that the thermal image based leak detection and localization method is effective and sensitive.

MODELING AND SIMULATION

There are mainly two types of heat transfer process happened when air leak occurred, one is heat absorption caused by air expansion from the leak namely Joule-Thomson effect, the other is heat transfer between air leak flow and leak hole in the vessel if the temperature of them are varied. So, the change in temperature around the leak will be the superposition by the two processes above.
From the aspect of physical quantity, the process of air leak can be considered as steady flow field coupled with two kinds of unsteady heat transfer.

Joule-Thomson Effect

In the course of throttle, gas temperature varies adapted to its pressure, namely Joule-Thomson effect. Normally, in the field of leakage detection with medium of compressed air, the temperature of medium is mostly from 250K to 350K, meantime the test pressure is lower than 1Mpa. Consequently air leak throttle makes positive Joule-Thomson effect according to the isenthalpic inversion curve in the Joule-Thomson T-P diagram. Leak air will have a temperature drop while passing through the leak hole, so it will absorb partial heat from the vessel, and then temperature of leak hole will decrease too. For the sake of calculating the quantitative temperature drop, Joule-Thomson coefficient u_j is introduced as following, which is defined as the temperature change rate in company with pressure during the throttle process (isenthalpic process)[2].

$$u_j = \left(\frac{\partial T}{\partial P}\right)_h = \frac{T\left(\frac{\partial v}{\partial T}\right)_P - v}{C_P} \tag{1}$$

Where, T is thermodynamic temperature of air, K; P is air pressure, Pa; v is specific volume of air, m^3/kg; C_p is specific heat at constant pressure, J/K·kg.
Eq(8) shows that, so long as $(\partial v/\partial T)_P$ is worked out from gas state equation and is substituted into Eq(8), u_j will be obtained. Then the temperature difference affected by leak flow will be obvious:

$$\Delta T = \int_{P_1}^{P_2} u_j dP \tag{2}$$

However, for most occasions, it is always computationally expensive to get $(\partial v/\partial T)_P$, therefore direct derivation to real gas state equation which mentioned in reference [3] has been done.
Van Der Waals (VDW) Equation is the primary way to describe real gas, as following:

$$P = \frac{RT}{v-b} - \frac{a}{v^2} \tag{3}$$

u_j will be obtained from simultaneous equations of Eq.(1) and Eq.(3):

$$u_j = \left(\frac{\partial T}{\partial P}\right)_h = \frac{R(v-b)v^3 - RTv^4 - 2av(v-b)^2}{[RTv^3 + 2a(v-b)^2]} \tag{4}$$

Where, R is molar gas constant, 287.1 N·m/(kg·K) for dry air; a and b are Van Der Waals constants, $a=135.8\times10^{-3}$ Pa·m^6/K·mol^2, $b=36.4\times10^{-3}$ m^3/K·mol.
Though the VDW Equation qualitatively describes the status of real gas, it is not so accurate in quantitative calculation, so compressibility factor Z is applied in the computation of u_j. After v is obtained by substituting the known variable T and P into correction state equation of ideal gas, u_j will be gotten.
Compressibility factor Z is determined by Dranchuk-Purvis-Robinson Correlative Equation[4]:

$$Z = 1 + \left(0.31506 - \frac{1.0467}{T_r} - \frac{0.5783}{T_r^3}\right)\rho_r + \left(0.5353 - \frac{0.6127}{T_r} + \frac{0.6185}{T_r^3}\right)\rho_r^2 \tag{5}$$

Where, $\rho_r=0.27(P_r/ZT_r)$ is relative density of air; $T_r=T/T_c$ is relative temperature of air; T_c is critical temperature, T_c=126K for air; $P_r=P/P_c$ is relative pressure of air; P_c is critical pressure, T_c=3.399 Mpa for air.

Heat Transfer Model

Using the thought of finite element method, the test vessel can be divided into a great deal of infinitesimal

surface elements. Concerning a variety of heat transfer processes among each element, environment, and the compressed air medium with low temperature, the heat transfer model is established. Assuming there is no high-temperature heat source around the test vessel, therefore thermal radiation effect can be ignored. Taking the adjacent infinitesimal element K and K+1 which are far smaller than the leak hole for instance, thermal convection and heat conduction have been considered, sketch is shown as following:

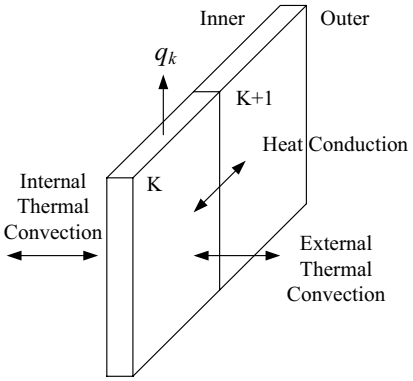

Figure 1 Sketch of heat transfer analysis

If the element K joins with leak hole, q_k is defined as the quantity of heat taken away by leak flow, for the result of forced convection effect.
Assume that λ is thermal conductivity, T_k and T_{K+1} are the temperatures of adjacent elements K and K+1 respectively, $A_{k,k+1}$ is the section area of thermal conduction, $L_{k,K+1}$ is effective length. Then the thermal conduction between element K and element K+1 can be described:

$$Conduction_{k,k+1} = -\frac{\lambda A_{k,k+1}}{L_{k,k+1}}(T_k - T_{k+1}) \qquad (6)$$

As the element K joins with n elements simultaneously, the total quantity of thermal conduction is represented as following:

$$Conduction = -\sum_n \frac{\lambda A_{k,k+n}}{L_{k,k+n}}(T_k - T_{k+n}) \qquad (7)$$

Thermal convection of every single infinitesimal element consists of two parts: the one between external surface and ambient; the other between internal surface and inner compressed air with low temperature. On the basis of Newton Law, assuming the surface area of element K is A_k, the temperature of element K is T_k, then the thermal convection can be conducted:

Interior surface: $Convection_{inside} = A_k\alpha_i(T_k - T_i)$ (8)

Exterior surface: $Convection_{outside} = A_k\alpha_o(T_k - T_o)$ (9)

Where, T_i is the temperature of compressed air inside the test vessel; T_0 is ambient temperature; α is convective heat transfer coefficient.
On the occasion of natural convection, α is a constant, while if there is forced convection, α will be a variable related to flow velocity, and can be conducted by some theoretical and empirical formulas. On account of natural convection happens in both inside and outside of the test vessel, so α_i and α_o are two constants.
From the analysis above, heat balance equation of element K is established as following:

$$\sum_n \frac{-\lambda A_{k,k+n}}{L_{k,k+n}}(T_{k+n} - T_k) + A_k\alpha_i(T_k - T_i) + A_k\alpha_o(T_k - T_o) + q_k = 0 \qquad (10)$$

Where, boundary condition q_k=0 exists in those elements which are nonadjacent with the leak hole. Setting up the heat balance simultaneous equations of all elements, temperature distribution of the test vessel will be obtained.

Finite Element Analysis

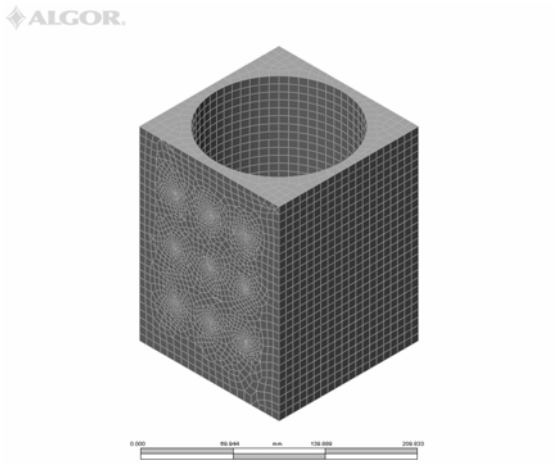

Figure 2 Meshed model

On the theoretical basis of (1) and (2), Simulation work is done below by using ALGOR finite element analysis software[5]. Taking general conditions of vessels' leakage detection for reference, and the material of sample model is chosen as 201.T4 sand cast aluminum. After CAD model is meshed (as shown in Figure2), initial temperatures of nodes are set to 298K, and more boundary conditions are listed in Table 1.

Table 1 Boundary conditions for simulation

Parameter	Internal air	Ambient
Type of Convection	Natural	Natural
Abs. Pressure (Mpa)	0.6	0.1
Temperature (K)	263	298
Mass Density (Kg/m^3)	7.94	1.18
Dynamic Viscosity (Pa·s)	1.67×10^{-5}	1.84×10^{-5}
Specific heat (J/kg·K)	1004	718
Thermal Conductivity (J/m·h·K)	84	94
Thermal Expansion Co-efficiency (1/K)	3.80×10^{-3}	3.36×10^{-3}

Dimension of the model is 150mm×150mm×200mm, internal columnar cavity has a radius of 67mm, and its height is 185mm. There are nine via holes composed of 3 rows 3 columns on the facade of the model, holes in each row have a same radius of 0.2mm, 1mm, 0.5mm respectively (from up to down), and holes in each column are in equal depth of 19.74mm，7.92mm，19.74mm respectively (from left to right).

Figure 2 shows the model after meshing with bricks and tetrahedral, because of the great differences in size between the hole and the vessel, some refinement points are defined round the simulated leak hole in order to keep precision.

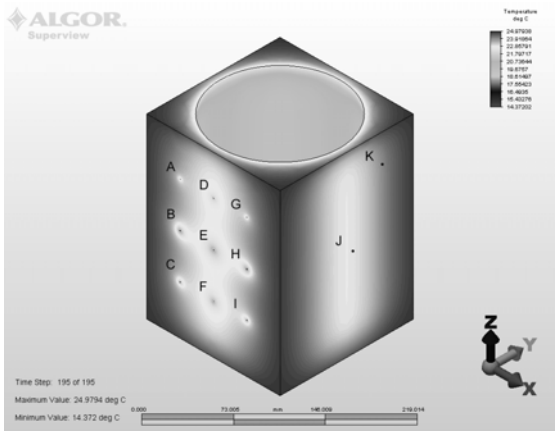

Figure 3 Temperature field of simulation

Figure 3 shows the temperature field of test vessel model when it reaches heat transient equilibrium. For the sake of research on the temperature difference, points A~I near the simulated leak hole and points J~K in no-leak region have been taken as the observational points. In virtue of the both effects of Joule-Thomson and heat exchange, a kind of annular distribution in temperature is presented around the simulated leak hole, and the more the leakage is, the bigger the radius of annular distribution is. Meanwhile, the smaller the depth of leak hole is, the greater the change in temperature gradient is.

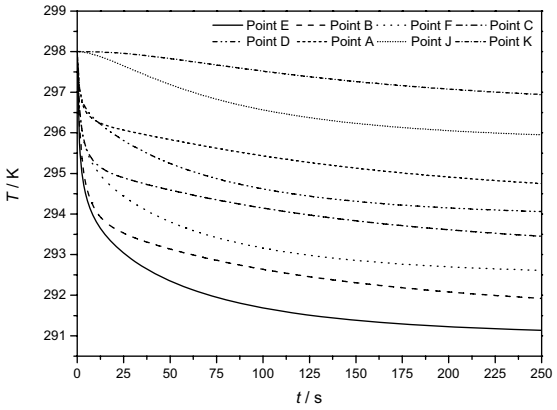

Figure 4 Curves of observational points

Simulation curves of observational points A~F and J~K are shown in Figure 4. From the curves, there is quick drop in temperatures of all the observational points near the leak hole when test starts, while 12 seconds later the tendency of change in temperatures becomes gentle. Since temperatures are steady inclined, the variety in depth of the holes affects the temperature gradient much distinctly. Besides, due to good thermal conductivity of sand cast aluminum, the decrease of temperatures of point J and K is approximate 1 K and 1.7 K respectively, but the changes are still far smaller than those in point A~F.

EXPERIMENT AND RESULTS

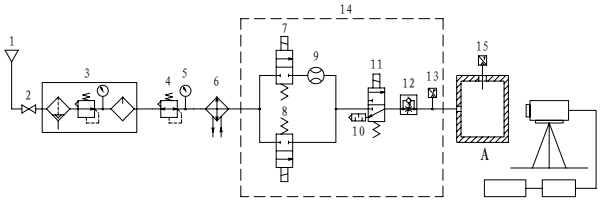

1: Air source 2: Stop valve 3: Pneumatic auxiliary components 4: Precision regulator 5: Pressure gauge 6: Freon based active cooler 7,8: Direct operated switch valve 9: Flow meter 10: Silencer 11: Two-position three-way valve 12: Speed control valve 13: Pressure sensor 14: Insulation material 15: Temperature sensor 16: Infrared camera 17: Computer 18: Image acquisition card A: Test vessel

Fig 5 Experimental pneumatic circuit

The experiment is carried out with the conditions: the test vessel is 500mL air volume with leak which is made of cast aluminum, measured leak flow rate is 20 sccm, inflation pressure is absolute 0.6 Mpa, temperature of compressed air is 263 K, and ambient temperature is

301 K.
Two thermal images are captured utilizing the pneumatic circuit [6] as shown in Figure 5, and Figure 6 (a) shows the temperature field of the air volume before inflation, while Figure 6 (b) shows the temperature field of air volume in the time of 60s after inflation.

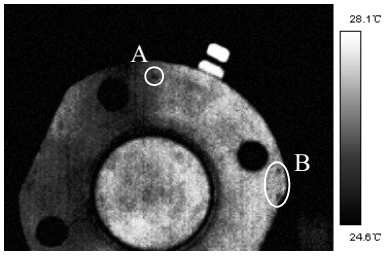

(a)Before inflation

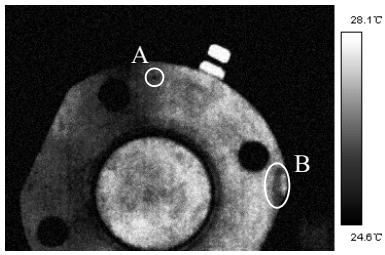

(b) 60s after inflation

Figure 6 Thermal images of air volume with leak

As the marks shown in Figure6 (a), three obvious singular temperature points can be seen in the regions A and B, among them, the one in region A is visible defect on the surface whereas the ones in region B are not, so all the three points are suspected to be the leak holes if without checking them in Figure6 (b). Comparing both the regions in Figure6 (a) and Figure6 (b), region A is invariant between the two images, while the region B in Figure6 (b) becomes darker than that in Figure6 (a). Hence a preliminary judgment can be made that the point in region A is not a leak hole but defect, nevertheless there are two invisible leak holes in region B. More accurate conclusion will be proposed in the following section by the use of leakage detection and localization method based on local entropy difference algorithm.

LOCAL ENTROPY DIFFERENCE ALGORITHM

Assume that image function has non-negative value, namely $f(x,y)>0$, for a image which size are M×N pixels, define:

$$E = -\sum_{r=1}^{M}\sum_{j=1}^{N} p_{ij} \log_2 p_{ij} \tag{11}$$

Where $$p_{ij} = f(i,j) / \sum_{i=1}^{M}\sum_{j=1}^{N} f(i,j) \tag{12}$$

The appearance probability of a certain gray value is characterized by p_{ij}, and E is named image entropy, furthermore if calculation is only done to one local area of the whole image, then it is called local entropy. According to the definition, entire amount of information contained in the whole or partial image can be reflected by entropy[7]. Because of the existence of negative sign in Eq. 11, so the richer the information is, the smaller the value of entropy is.
In the application of leakage detection and localization based on infrared thermography, leak will be embodied in the images, that is, leak adds some information into thermal images, and it is proved by the experiment shown in Figure 6. Back to the definition, merit is found that even though there is geometric distortion in partial images sometimes, the local entropy is invariant for its statistical characteristics. Moreover, the entropy depends on the computation of whole area, so its robustness may not be influenced by several singular values of isolated pixels. Meanwhile, its anti-noise advantage is ensured by normalization processing of p_{ij}.
Due to logarithm involved, sometimes Eq.1 will be simplified as following by taking Taylor Expansion, in order to get real-time performance improvement.

$$E_f = -\sum_{r=1}^{M}\sum_{j=1}^{N} p_{ij}(p_{ij} - 1) \tag{13}$$

Where $$p_{ij} = f(i,j) / \sum_{i=1}^{M}\sum_{j=1}^{N} f(i,j) \tag{14}$$

From the perspective of evaluation, entropy, as the characteristic measurement parameter of image information, provides a set of scientific means to evaluate the degree of leakage. Therefore, local entropy difference algorithm is adopted, and its strategies are described below.
For a thermal image F of test vessel captured before inflation, which size are M×N pixels, F will be traversal scanned firstly by an $n_1 \times n_2$ template named A. At the same time, absolute values of every local entropy based on A will be calculated and saved. When the scanning work is done, a matrix $E_F(n_1,n_2)$ is obtained, and all the local entropies are stored in the matrix orderly. Then same calculation will be applied to the thermal image G which is captured in a certain time delay after inflation, and its size are M×N pixels too, similar matrix $E_G(n_1,n_2)$ will be gotten sequentially. Afterward, the difference of local entropy matrix $\Delta E(n_1,n_2)=|E_F - E_G|$ is computed and $\Delta E(n_1,n_2)$ becomes the critical factor for leakage detecting and locating consequently.
(1) If thermal image G matches F well, then the value of ΔE will approach zero, hereby a conclusion can be

made that there is no leak in the test vessel.
(2) Setting the threshold δ as the criteria, if there is a salient region in the local entropy matrix of image, and the value of $\Delta E(n_1,n_2)$ in that region is tenably greater than δ, then leak is confirmed (probably not only one region).
(3) Calculation of reverse mapping is executed to the salient region of local entropy matrix $\Delta E(n_1,n_2)$, so that the coordinates of leakage point can be obtained subsequently.
By using upper strategies, local entropy matrixes with absolute values of the two thermal images shown in Figure 6 are calculated, and are presented in Figure 7 (a) and Figure 7 (b) respectively, finally the difference matrix between them can be easily gotten, as shown in Figure 8 (c).

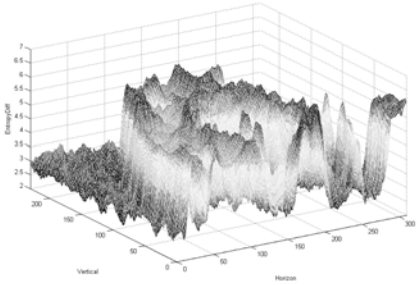

(a) Absolute local entropy matrix of Figure 6 (a)

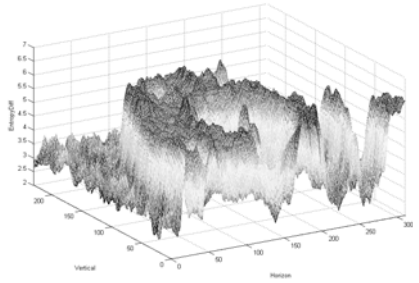

(b) Absolute local entropy matrix of Figure 6 (b)

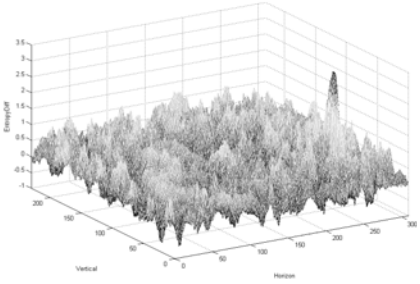

(c) Difference matrix between (a) and (b).

Figure 7 Local entropy matrixes

As shown in Figure 8 (c), the singular value in matrix fits the leakage point well, and the adoption of local entropy difference algorithm eliminates the shape information of test vessel effectively. After operation, the contrast between leak area and non-leak area gets much more obvious, meanwhile noise and geometric distortion of the thermal images are suppressed evidently.

CONCLUSON

The leakage detection and localization method based on infrared thermography for the vessels is proposed in this paper, and it is proved to be feasible by simulating and experimental results. Mathematical model has been established for heat transfer, and it is evident that the differences in temperature caused by leak are conspicuous enough to be detected, especially by the use of compressed air of low temperature are. Moreover, speed optimization of local entropy difference algorithm should be done in the further study for its computational complexity.

REFERENCES

1. Xiaojian, Wu and Rongxin, Yan, Leak Detection, China Machine Press, Bei Jing, 2005, pp. 49-50, 81-84, 146-148.
2. Maric. I., The Joule-Thomson effect in natural gas flow-rate measurements, Flow Measurement and Instrumentation, 2005, 16-6, pp. 387-395.
3. Shini, Peng and Jianlun Chen, Calculation for Temperature Drop Induced by Adiabatic Throttle of Natural Gas, Gas & Heat, 2006, 26-1, pp. 1-4.
4. ter Brake, H.J.M. and Wiegerinck, G.F.M., Thermodynamic optimization of sorption-based Joule-Thomson coolers, Cryogenics, 2007, 47-3, pp. 143-152.
5. Gonzalez Ulises, Modeling and simulating MEMS devices using finite element analysis, Proceedings of 2001 ASME International Mechanical Engineering Congress and Exposition, New York, NY, United States, pp. 2583-2587.
6. Terumi Inagaki and Yoshizo Okamoto, Diagnosis of the leakage point on a structure surface using infrared thermography in near ambient conditions, NDT&E international, 1997, 30-3, pp. 135-142.
7. Chi Zhang and Hongbin Zhang, Detecting digital image forgeries through weighted local entropy, Proceedings of 2007 IEEE International Symposium on Signal Processing and Information Technology, Piscataway, NJ, USA, pp. 62-67.